



IAU-ARAK

J. Iran. Chem. Res. 4 (2011) 199-206

Journal of the
Iranian
Chemical
Research

www.iau-jicr.com

Synthesis of Nano-Ca doped Ceria by combustion method and investigating of effective factors on process

Ali Ainirad *

Department of chemistry, University of Science and Technology of Iran, Tehran, Iran

Received 12 June 2011; received in revised form 2 September 2011; accepted 10 September 2011

Abstract

A Synthesis of doped ceria by combustion method is performed. Two types of fuel such as urea and glycine is used to investigate the effect of fuel reactivity and reaction rate on the morphology of the resulted powders. Thermo gravimetric analysis is carried out by (TG/DTA, Rigaku Thermalplus TG 8120) to study the exo–endo temperature of as-received powder. The crystalline phases are identified by X-ray diffraction analysis (XRD). The average crystallite size, D , is estimated by using the Scherrer formula about 40nm. The calculated lattice parameter is 5.44Å. A FT-IR study is carried out on the obtained gel and reveals that a Glycine-Metal complex is formed in alkaline conditions which help in preventing metal ions selective precipitation and in maintaining the compositional homogeneity of the resulted powder. Finally, the effect of pH value, in the primary solution, and fuel type on the powder characteristics such as lattice parameter and morphologies are described.

Keywords: Solid oxide fuel cell; Nano Ceria; Combustion method; pH value.

1. Introduction

Solid oxide fuel cell (SOFC) has attracted much attention in recent years because of its high-energy conversion efficiency and environmental friendship. In fact, solid oxide fuel cells (SOFCs) are electrochemical devices that convert the chemical energy of a fuel into electrical energy in a clean, cheap and efficient way and Consist of three parts, including anode, cathode and electrolyte [1]. Conventional SOFCs which use yttria-stabilized zirconia (YSZ), as an electrolyte, are operated at around 1273K. However, such high temperatures often lead to some problems such as solid-state reactions between the components, thermal degradation and thermal expansion mismatch. It becomes increasingly important to reduce the operating temperature of the SOFC [2].

In recent years, there has been an increasing interest in the synthesis of nanocrystalline metal oxides due to important applications in advanced ceramics [3-9]. Nanocrystalline of doped ceria is a potential electrolyte material for IT-SOFCs because of its much higher oxygen ionic conductivity than YSZ [10-11]. Ceria itself is not a good ionic conductor, but ionic conductivity increases significantly with the introduction of oxygen vacancies caused by doping of ceria with two or more components at the same time and the research results showed that complex doping

* Corresponding author. Tel.: +98 919 2512130.

E-mail address: aliainirad@yahoo.com (A. Ainirad)

with several rare earth or/and alkali earth elements was an effective method to improve the ionic conductivity of the electrolyte [12-15].

In the past few years, combustion synthesis of multi component ceramic oxides has been gaining reputation as a straightforward preparation process to produce homogeneous, very fine, crystalline and unagglomerated powders, without the intermediate decomposition and or calcining step [16-17]. The basis of the combustion synthesis technique comes from the thermo chemical concepts used in the field of propellants and explosives [18].

As we know, the nature of the fuel and the pH of the starting solution are important factors in preventing selective precipitation and/or phase separation during the evaporation of solvent, which may result in phase and compositional inhomogeneities [19-21] For example, Pathak et al. [22] found that the pH values in precursor solutions have important effect on the morphologies of nanocrystalline alumina powder produced by citrate–nitrate combustion synthesis.

The zwitterionic character of glycine can effectively complex various metal ions which help in preventing their selective precipitation and therefore in maintaining the compositional homogeneity among the constituents during the evaporation of solvent. Namely, metal nitrates with glycine as complexing agent are highly promising in producing various amorphous and nanocrystalline ceramic powders [21, 23-29]. The solution-based combustion technique using glycine has been studied widely, such as the effect of the fuel-to-oxidant ratio on the powder characteristics [24, 30]. However, only a few efforts have been made to investigate the effects of the pH on the glycine–nitrate combustion synthesis of doped ceria. In this paper, solution-based combustion synthesis is applied to prepare the nanocrystalline powders of doped ceria. The effect of pH values in the precursor solutions and the fuel type on the powder characteristics such as crystallite size, lattice parameter and morphologies are described.

2. Experimental

In present work we synthesized doped ceria by combustion method. Cerium nitrate and calcium nitrate was used as the metal source and also as the oxidant. Urea and glycine was used as the two types of fuel to investigate the effect of fuel reactivity and reaction rate on the morphology of the resulted powders.

As reported in our previous work [30], based on propellant chemistry, in order to release the maximum energy, the fuel to oxidant ratio must be 1 but since thermal decomposition of some nitrates at 250 °C causes to decreasing amount of oxidant at the moment of combustion thus, the most of the energy is obtained through combustion by deficient fuel ratio (i.e. fuel to oxidant ratio = 0.8). It suggests that, reaching to 1 mol of $Ce_{1-y}Ca_yO_{2-y}$ needs to $0.8*((15-5y)/9)$ mol of glycine or $0.8*((15-5y)/6)$ mol of Urea.

According to the above, to reach to 1 mmol of $Ce_{0.9}Ca_{0.1}O_{1.9}$, 0.391 g of cerium nitrate and 0.023g of calcium nitrate and 0.080g of urea, or 0.066g of glycine instead of urea, were dissolved in double distilled water then pH value of the solution was adjusted by adding ammonium hydroxide. The obtained translucent solution was heated at 80 °C until it turned into a viscose gel. The heating was continued up to 300 °C and after auto-ignition a white and voluminous powder was produced. During the ignition, the container must be covered with a fine-mesh sieve to prevent the powder from flying out of its container. Finally the resulted powder was calcined at 600 °C for 3h.

Thermogravimetry (TG/DTA, Rigaku Thermalplus TG 8120) were used to study the exo-endo temperature of as-received powder. A heating rate of 10 °C min⁻¹ was used in TG measurements up to 1000°C in air. The crystalline phases were identified by X-ray diffraction analysis (XRD) by using X-ray diffractometer (Siemens D5000) and Cu K_β radiation ($\lambda = 0.15418$ nm). The average crystallite size, D, was estimated by using the Scherrer formula: $D = (0.9\lambda)/(\beta \cos\theta)$ [31] Which, β is the line broadening measured at half of height of peak, θ is the angle of reflection and λ is the wavelength of radiation.

The lattice parameters were calculated by using formula that is shown in below:

$$1/d_{hkl}^2 = h^2/a^2 + k^2/b^2 + l^2/c^2 \quad [32]$$

which, d is the interplanar distance, (h, k, l) are the miller indices for the corresponding d -spacing and a, b, c are the lattice parameters. Scanning electron microscopy (SEM) was used to morphological studies.

3. Results and discussion

3.1.1. Phase structure

XRD pattern of the calcined powder at 600°C is shown in Fig. 1 that indicates the presence of a cubic fluorite type structure. This suggests that alkaline earth oxides are dissolved into the ceria. The position of XRD diffraction peaks also is moved toward lower angles compared to pure ceria. The average crystallite size, D , is estimated by using the Scherrer formula about 40nm and the calculated lattice parameter was 5.44 Å, which was in well agreement with the reported values. However, the peaks are relatively broad, which indicates the presence of nanocrystalline phase. The average crystallite size, determined by the Scherrer equation, was 40 nm. This was in good agreement with Scanning Electron Microscopy results on the same material.

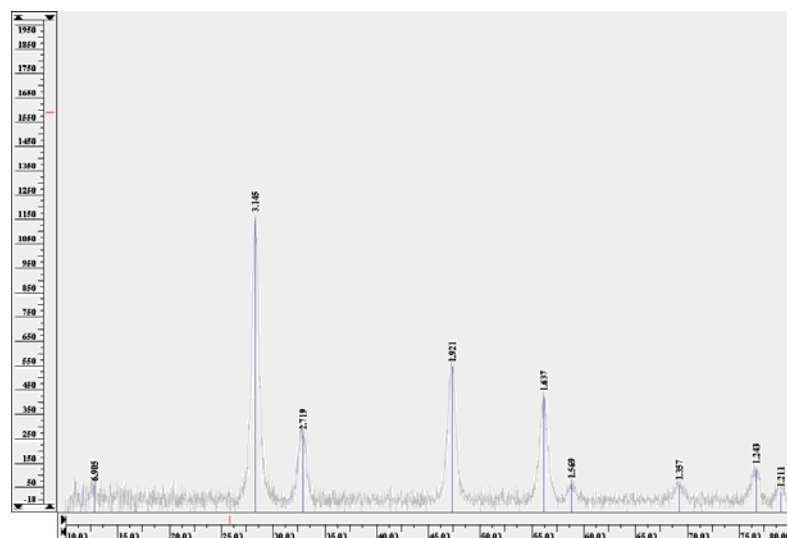


Fig. 1. XRD pattern of the calcined $Ce_{0.9}Ca_{0.1}O_{1.9}$ powder.

3.1.2. Investigating of TGA analysis

The TGA curve of the as-synthesized powder in oxygen atmosphere is shown in Fig. 2. The TG plot has shown a weight loss between 100-200 °C that is duo to water loss. Next weight loss in 250-400 °C maybe is related to the combustion of residual organic matter and finally at 750 °C again a weak weight loss is due to decomposition of calcium carbonate or calcium hydroxide [33].

3.2. Investigating effective factors on the combustion process

Many factors are effective on the various steps in the combustion process and properties of the resulted powder. To understand how the process changes by these factors, we synthesized several samples in different conditions, for example, we changed the pH value of the starting

solution and we studied the compositional homogeneities of the resulted powder. In following we'll investigate some of these factors (such as pH value and rate of reaction).

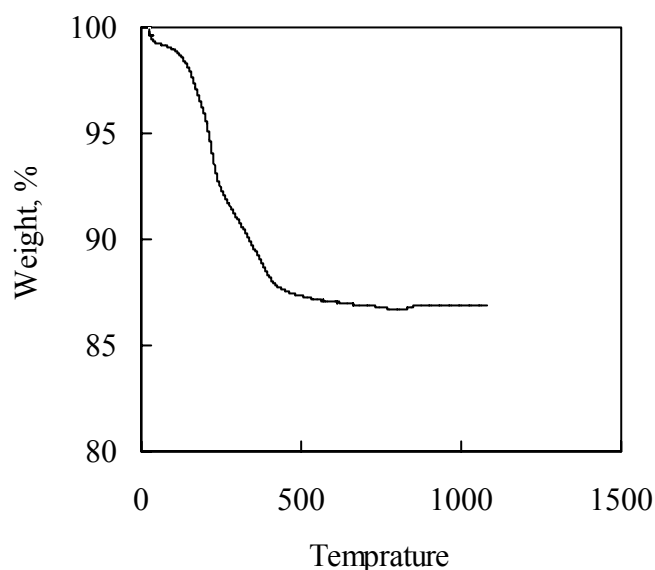


Fig. 2. TGA curve of the as-synthesized powder.

3.2.1. Investigating the effect of precursor's pH

As we know, glycine is an aminoacidemia that has two functional group (amine & carboxylic). Because of zwitterionic character, the glycine is able to forming various metal ions complex which helps in preventing their selective precipitation and therefore in maintaining the compositional homogeneity among the constituents. Namely, metal nitrates with glycine as complexing agent are highly promising in producing various amorphous and nanocrystalline ceramic powders [21, 23-29].

Thus, we studied on chemical structure of pure glycine, dry gel which was formed in alkaline condition and dry gel from primary solution, including glycine and metal nitrates, without pH adjustment.

Figs. 3 shows FT-IR spectrum of dry gels from primary solution a) without pH adjustment b) adjusted pH value at 8.3 and c) pure glycine. As can be seen, IR spectrum of pure glycine has shown peaks which are related to NH_4^+ ($>2800\text{ cm}^{-1}$) and COO^- (1600 & 1411 cm^{-1}) and thus clearly reveals two ionic structure for it.

Fig. 3a shows presence of NO_3^- (1420 & 1458 cm^{-1}) and COO^- (1606 & 1415 cm^{-1}) groups and the peak which is related to NH_4^+ is shifted to $>3200\text{ cm}^{-1}$. Based on these data, there is no chemical interaction between functional groups in a mixture of glycine and metal ions without pH adjustment.

But in IR spectrum of dry gel which is formed in alkaline condition, Fig 3b, as can be seen, the sharp peak which is related to COO^- group is shifted to 1608 cm^{-1} and also is broader than that of free COO^- group due to interaction between glycine and metal ions and because of the glycine-metal complex formation. Formation of this complex probably helps in preventing selective precipitation of metal ions and in increase the compositional homogeneity of the resulted powder.

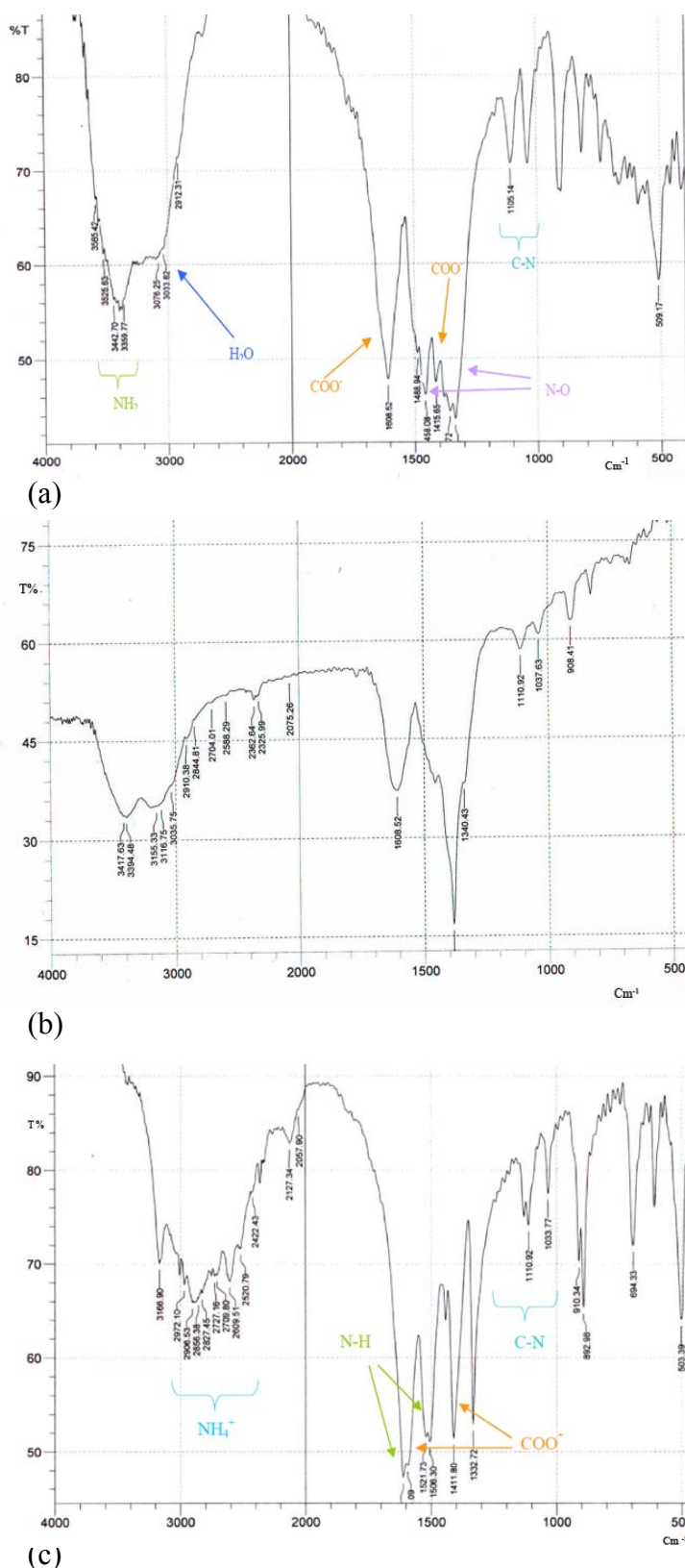


Fig. 3. FT-IR spectrum of a) dry gel a from primary solution without adjusting on pH b) dry gel which formed in alkaline condition and pH adjusted at 8.3 and c) pure glycine.

Fig. 4 shows lattice parameters of $Ce_{0.9}Ca_{0.1}O_{1.9}$ versus the pH values of the starting solution. As can be seen, the lattice parameter reaches maximum value at pH 7.5. Since the ionic radius of Ca^{2+} (0.126 nm) is larger than ionic radius of Ce^{+4} (0.1019nm), it is reasonable that the increase of lattice parameter is because of the M-G complex formation at pH 7.5 which causes to

preventing calcium ions selective precipitation and thus, because of more entry calcium ions into the lattice of ceria, the lattice parameter of resulted powder is increased.

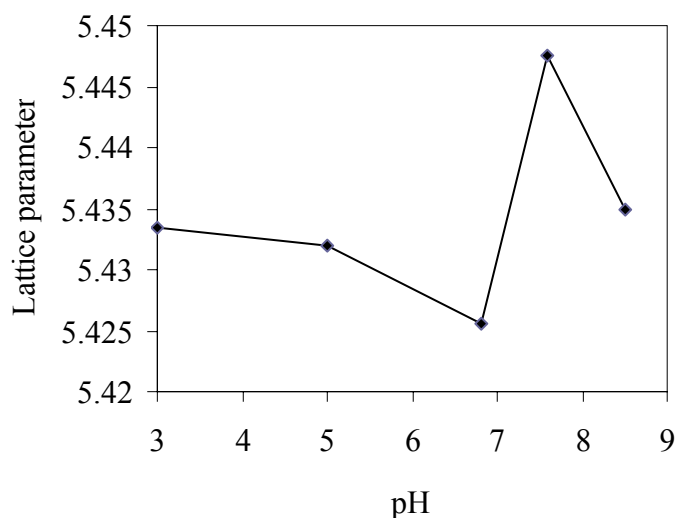


Fig. 4. Variations of lattice parameter $Ce_{0.9}Ca_{0.1}O_{1.9}$ versus pH.

On the other hand, decrease of lattice parameter at pH 8.5 and 6.8 is due to calcium hydroxide precipitation during the solvent evaporation in the absence of M-G complex. These observations are agreement with FT-IR results. According to the above, pH adjustment in the primary solution through the M-G complex formation can help in maintaining the compositional homogeneity of the resulted powder.

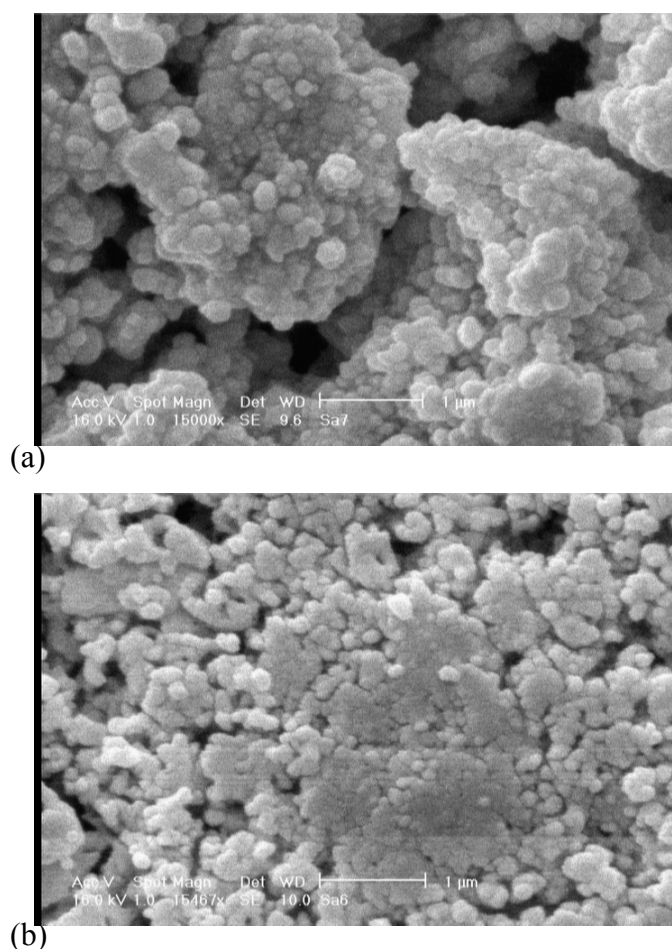


Fig. 5. a) SEM micrograph of powder synthesized by a) urea b) glycine.

3.2.2. Investigating of the type of fuel

Both, reaction rate and amount of released gases during the combustion are effective on morphology of the synthesized powder. Since the number of gas moles which is released during the combustion of urea is more than glycine, we expected that the obtained powder from urea is softer and has less agglomerations but the reaction rate of urea was much less than glycine so that the released gases of urea was not able to break the agglomerates. This issue is well shown in Fig. 5. Fig. 5a shows SEM micrographs of synthesized powder by urea, as the fuel, and Fig. 5b shows micrographs of synthesized powder by glycine. As can be seen, the size of agglomerates in (a) is much larger than (b), that is due to the slower reaction of urea compared to glycine. This reveals the effect of fuel reactivity and reaction rate in the combustion synthesis.

4. Conclusion

In this work we synthesized Nano-doped ceria by combustion method. As we observed in FT-IR results, the sharp peak which is related to COO⁻ group, because of interaction between glycine and metal ions, shifted to 1608 cm⁻¹ and was broader than that of free COO⁻ group. The lattice parameter of the resulted powder also reached a maximum value at pH 7.5 due to M-G complex formation and preventing from metal ions selective precipitation at this pH value. Metal hydroxide precipitations at pH 8.5 and 6.8 also caused to decrease of lattice parameter. Finally it also observed that, although the amounts of released gases for urea were more than glycine, but because of the slower reaction of urea, the released gases was not able to break the agglomerates.

References

- [1] X. Hongmei, Y. Hongge, Ch. Zhenhua, *Solid State Sciences* 10 (2008) 1179-1184.
- [2] J.V. herle, T. Kawada, N. Sakai, *Solid State Ionics* 86-88 (1996) 1255-1258.
- [3] C.H. Shek, J.K. L. Lai, T.S. Gu, G. M. Lin, *Nanostruct. Mater.* 8 (1997) 506-610.
- [4] A. Janbey, R.K. Pati, S. Tahir, P. Pramanik, *J. Eur. Ceram. Soc.* 21 (2001) 2285-2289.
- [5] L.C. Pathak, T.B. Singh, S. Das, A.K. Verma, *Mater. Lett.* 57 (2002) 380-385.
- [6] J.J. Kingsley, K.C. Patil, *Mater. Lett.* 6 (1988) 427-432.
- [7] R.H.G.A. Kiminami, M.R. Morelli, *Am. Ceram. Soc. Bull.* 79 (2000) 63-67.
- [8] Y.Q. Wu, Y.F. Zhang, X.X. Huang, J.K. Guo, *Ceram. Int.* 27 (2001) 265-268.
- [9] V.V. Karasev, A.A. Onishchuk, *Combust. Explos. ShockWave* 37 (2001) 734-736.
- [10] B.C.H. Steele, *Solid State Ionics* 129 (2000) 95-110.
- [11] H. Inaba, H. Tagawa, *Solid State Ionics* 83 (1996) 1-16.
- [12] J. Herle, D. Seneviratne, A.J. McEvoy, *J. Eur. Ceram. Soc.* 19 (1999) 837-841.
- [13] F.Y. Wang, S. Chen, S. Cheng, *Electrochem. Commun.* 6 (2004) 743-746.
- [14] F.Y. Wang, S. Chen, Q. Wang, S.X. Yu, S. Cheng, *Catal. Today* 97 (2004) 189-194.
- [15] D.A. Fumo, M.R. Morelli, A.M. Segadaes, *Mater. Res. Bull.* 31 (1996) 1243-1255.
- [16] D.A. Fumo, J.R. Jurado, A.M. Segadaes, *Mater. Res. Bull.* 32 (1997) 1459-1470.
- [17] J.R. Jain, K.C. Adiga, V.R.P. Verneker, *Comb. Flame* 40 (1981) 71-79.
- [18] R.D. Purohit, S. Saha, A.K. Tyagi, *J. Nucl. Mater.* 288 (2001) 7-10.
- [19] T.V. Anuradha, S. Ranganathan, T. Mimani, *Scripta Mater.* 44 (2001) 2237-2241.
- [20] T. Mimani, *J. Alloys Compd.* 315 (2001) 123-128.
- [21] L.C. Pathak, T.B. Singh, S. Das, A.K. Verma, *Mater. Lett.* 57 (2002) 380-385.
- [22] T.Y. Peng, H.P. Yang, X.L. Pu, B. Hu, Z.C. Jiang, *Mater. Lett.* 58 (2004) 352-356.
- [23] R.D. Purohit, S. Saha, A.K. Tyagi, *J. Nucl. Mater.* 288 (2001) 7-10.
- [24] N. Dasgupta, R. Krishnamoorthy, K.T. Jacob, *J. Inorg. Mater.* 3 (2002) 143-149.
- [25] T. Mimani, K.C. Patil, *Mater. Phys. Mech.* 4 (2001) 1-5.
- [26] T.V. Anuradha, S. Ranganathan, T. Mimani, *Scripta Mater.* 44 (2001) 2237-2241.
- [27] G. Fagherazzi, S. Polizzi, M. Bettinelli, A. Speghini, *J. Mater. Res.* 15 (2000) 586-589.
- [28] D.G. Lamas, R.E. Juarez, G.E. Lascalea, *J. Mater. Sci. Lett.* 20 (2001) 1447-1449.
- [29] A. Ainirad, M. M. Kashani-Motlagh, A. Maghsoodipoor, *J. Alloys Compd.* 509 (2011) 1505-1510
- [30] B.D. Cullity, *Elements of X-Ray Diffraction*, Addison-Wesley, Reading, MA, 1956.

- [31] P. Dattaa, P. Majewski, F. Aldinger, *Mater. Charact.* 60 (2009) 138-143.
[32] M. Yan, T. Mori, F. Yea, D. R. Ou, *J. Eur. Ceram. Soc.* 28 (2008) 2709–2716.